

An *in vivo* study on sonodynamic effects mediated by nanomicelles containing PpIX as a sonosensitizing agent

Maryam Bakhshizadeh ¹, Mehdi Hoseini ^{1, 2}, Samaneh Soudmand Salarabadi ³, Naser Tayebi-Meybodi ⁴, Ameneh Sazgarnia ^{3, 5*}, Bahareh Khalili Najafabad ^{6*}

¹ Department of Radiology Technology, School of Paramedical Sciences, Torbat Heydariyeh University of Medical Sciences, Torbat Heydariyeh, Iran

² Research Center of Advanced Technologies in Medicine, Torbat Heydariyeh University of Medical Sciences, Torbat Heydariyeh, Iran

³ Medical Physics Research Center, Basic Sciences Research Institute, Mashhad University of Medical Sciences, Mashhad, Iran

⁴ Department of Pathology, Faculty of Medicine, Mashhad University of Medical Sciences, Mashhad, Iran

⁵ Department of Medical Physics, Faculty of Medicine, Mashhad University of Medical Sciences, Mashhad, Iran

⁶ Department of Biomedical Engineering and Medical Physics, School of Medicine, Shahid Beheshti University of Medical Sciences, Tehran, Iran

ARTICLE INFO

Article type:

Original

Article history:

Received: Aug 14, 2025

Accepted: Nov 17, 2025

Keywords:

Breast neoplasms

Micelles

Nanoparticles

Protoporphyrin IX

Therapeutic ultrasound

Ultrasonic waves

ABSTRACT

Objective(s): Sonodynamic therapy (SDT) is a promising non-invasive adjuvant approach for treating accessible tumors, requiring ultrasound (US) waves, sonosensitizing molecules, and oxygen. However, sonosensitizers such as protoporphyrin IX (PpIX) face limitations, including poor water solubility, phototoxicity, and lack of targeting. To address these issues, we encapsulated PpIX in biocompatible nanomicelles to enhance solubility, reduce side effects, and improve tumor targeting.

Materials and Methods: After synthesizing, characterizing, and assessing the cytotoxicity of PpIX-loaded nanomicelles, the optimal concentration was selected. The 4T1 cell line was used to create a breast tumor model in BALB/c mice. To investigate the effect of SDT mediated by PpIX-loaded nanomicelles, tumors were exposed to US at 800 and 2400 kHz simultaneously, 10 min after intratumoral injection of the drug. The tumors were measured with a digital calliper, and tumor volume was calculated at specific time intervals and compared. The tumor tissue necrosis percentage was determined by pathological examination, and the volume loss in different groups was quantified.

Results: SDT with PpIX nanomicelles significantly reduced tumor volume within 7 days compared with controls ($P<0.05$), with the greatest volume loss observed in this group. Pathological analysis confirmed extensive tumor necrosis.

Conclusion: PpIX-loaded nanomicelles enhance SDT efficacy in breast tumors, demonstrating potential as a targeted delivery system. Repeated treatments may further inhibit tumor growth.

► Please cite this article as:

Bakhshizadeh M, Hoseini M, Soudmand Salarabadi S, Tayebi-Meybodi N, Sazgarnia A, Khalili Najafabad B. An *in vivo* study on sonodynamic effects mediated by nanomicelles containing PpIX as a sonosensitizing agent. Iran J Basic Med Sci 2026; 29: 225-230. doi: <https://dx.doi.org/10.22038/ijbms.2025.90437.19489>

Introduction

Cancer is one of the serious public health problems worldwide. According to global demographic indicators, the incidence of cancer is predicted to increase in the next few decades (annually, more than 20 million new cases of cancer by 2025). Common methods of cancer treatment include surgery, chemotherapy, and radiotherapy. Some of the serious problems with these methods include systemic toxicity and side effects (1-3). Among these, breast cancer constitutes approximately one-third of all malignancies in women, and its mortality rate is about 15% of all diagnosed cases (4). Therefore, there is a need for a completely selective and non-invasive treatment. Given this issue, SDT is a candidate that can be considered alone or in combination with other treatments (3-6). Among its advantages are a greater penetration depth than photodynamic therapy

(PDT), its non-ionizing nature, reduced side effects compared to radiation therapy, and its non-invasiveness (7, 8).

The most important tumor destruction mechanisms in SDT include cavitation, production of free radicals, and mechanical and thermal injuries (9). Cavitation caused by ultrasound waves leads to the formation of microbubbles in tissue fluids in a short period of time. Cavitation is classified into two categories: inertial and non-inertial. Inertial cavitation occurs in the presence of low-intensity acoustic waves. In fact, the intensity of these waves is not sufficient for the collapse of bubbles, and microbubbles oscillate continuously around an equilibrium radius in the presence of a sound field. At low frequencies and high intensities, transient cavitation occurs, with microbubbles oscillating, expanding, and collapsing, generating shock and shear waves that exert destructive effects on the tumor. When the intensity of ultrasound waves is sufficient to collapse

*Corresponding authors: Ameneh Sazgarnia. Medical Physics Research Center, Mashhad University of Medical Sciences, Mashhad, Iran. Email: sazgarniaa@mums.ac.ir; Bahareh Khalili Najafabad. Department of Biomedical Engineering and Medical Physics, School of Medicine, Shahid Beheshti University of Medical Sciences, Tehran, Iran. Email: Baharekhali389@gmail.com



© 2026. This work is openly licensed via CC BY 4.0.

This is an Open Access article distributed under the terms of the Creative Commons Attribution License (<https://creativecommons.org/licenses/by/4.0/>), which permits unrestricted use, distribution, and reproduction in any medium, provided the original work is properly cited.

microbubbles, sonoluminescence may occur, leading to sono-toxic effects on cancer cells. Additionally, heat generated by cavitation can lead to the formation of free radicals, which play a fundamental role in cellular damage (10). *In vitro* and *in vivo* studies suggest that dual-frequency ultrasound increases cavitation efficiency by creating a more irregular environment than single-frequency ultrasound (11, 12). Furthermore, studies indicate that nanoparticles or nanomicelles, acting as nucleation sites for cavitation, lower the cavitation threshold, enabling effective outcomes at low intensities while preserving healthy tissue. We can mention that the selection of 800 and 2400 kHz ultrasound frequencies was both experimentally motivated and clinically feasible. They fall within the range used by standard physiotherapy ultrasound machines, thus susceptible to possible clinical application. In addition, previous studies have shown that simultaneous exposure to a low (800 kHz) and high (2400 kHz) frequency enhances cavitation performance through acoustic interference, with improved microbubble instability, ROS production, and tumor cell killing compared to single-frequency exposure. Therefore, in this study, using twin frequencies was intended to optimize the therapeutic efficacy of sonodynamic therapy (SDT) without exceeding clinically applicable levels (13). In SDT, the presence of three elements, including ultrasound waves, sonosensitizer, and oxygen, is essential (10). Most sonosensitizers respond to ultrasound frequencies between 0.2 and 3 MHz (14). Many photosensitizers can also be used as sonosensitizers. Acoustic sensitizers have disadvantages, including low water solubility, phototoxicity, limited targeting ability, and short circulation times in physiological environments, which have limited their clinical applications (12, 15). Given these limitations, there is a need for a drug carrier system with high biocompatibility and tumor-specificity, which can be used in clinical work to target cancer cells and address these limitations.

Among drug delivery systems based on nanotechnology, such as liposomes, nanotubes, and nanomicelles, nanomicelles offer distinct advantages for cancer treatment, including high drug loading capacity and a small size that allows deeper penetration into tumor tissues and increases bioavailability. Micelles are used to encapsulate poorly soluble drugs. In addition to increasing drug solubility through their outer hydrophilic layer, they prevent detection and capture by the reticuloendothelial system (RES), thereby increasing the drug's circulation time in the biological environment.

Studies utilizing micelles loaded with sonosensitizers in SDT have demonstrated increased stability, uniform distribution of the sonosensitizer, and significant reduction in cell viability (16, 17). So, the sonosensitizer can be enclosed inside a micellar system so that, in addition to greater solubility in water, reduction of unwanted side effects, increase in biocompatibility, and their accumulation in the tumor, they have a better distribution (18).

In the present study, protoporphyrin IX (*PpIX*) was selected as a sonosensitizer, and to increase its water solubility, it was encapsulated in nanomicelles. And then the effect of SDT using *PpIX*-containing nanomicelles under simultaneous ultrasound irradiation at 800 kHz and 2400 kHz (frequencies available in physiotherapy devices) on a breast tumor model in BALB/c mice was investigated.

Materials and Methods

Materials

PpIX disodium salt (molecular weight [MW] 606.62

g·mol⁻¹), Roswell Park Memorial Institute (RPMI) medium 1640, Thiazolyl blue (MTT), trypsin-EDTA, trypan blue, penicillin/streptomycin, Phosphate-buffered saline (PBS), dimethyl sulfoxide (DMSO), Span 80 (MW 428.6 g·mol⁻¹) and Tween 80 (MW 1310 g·mol⁻¹) were obtained from Sigma-Aldrich (St. Louis, MO, USA). Fetal bovine serum (FBS) was procured from Gibco (Invitrogen Corporation, Carlsbad, CA, USA). All other chemicals were of analytical grade.

Synthesis and characterization of *PpIX*-loaded nanomicelles

Due to the high tendency of porphyrin dyes to form aggregates and dimers in aqueous solutions (19), they require a suitable encapsulation system to increase the quantum yield of the excited state and, as a result, singlet oxygen generation efficiency. At this stage, *PpIX*-loaded nanomicelles were prepared using a thin-film hydration method followed by sonication, as previously reported with minor modifications (20). Briefly, 20 mg of surfactant mixture (proportion 2:1 w/w, which corresponded to 6.66 mg of Tween 80 and 13.34 mg of Span 80) was dissolved in 3 mL of ethanol in a round-bottom flask. *PpIX* (5 mg, 25 % w/w of total surfactants) was dissolved in 1 mL of ethanol and added to the surfactant solution. The ethanol was evaporated via rotary evaporation for approximately 30 min to form a thin film, which was then dried overnight under vacuum. The film was subsequently hydrated with 2 mL of deionized water, sonicated for 5 min in an ice bath, and filtered through 0.22 µm RC membrane filters to remove unloaded *PpIX* or potentially large aggregates. The photosensitizer concentration in the resulting nanomicelles was determined via UV-vis spectroscopy after 20-fold dilution with deionized water. After formulation preparation, the UV-Vis absorption spectra and size distribution of the synthesized nanomicelles were characterized using a spectrophotometer (UNICO 2100-UV, China) and an SZ-100 instrument (HORIBA, Japan), respectively.

Cell line and *in vitro* cytotoxicity assessment of *PpIX*

The 4T1 murine mammary carcinoma cell line was obtained from the Pasteur Institute of Iran (Tehran) cell bank, certified for authenticity and contamination-free status. The 4T1 model was selected due to its clinicopathological resemblance to human triple-negative breast cancer, including rapid primary tumor growth and similar metastatic patterns. The cell line was kept in RPMI-1640 culture medium and 10% FBS at 37 °C and 5% CO₂. The culture medium was changed every 48 hr. RPMI-1640 and FBS were purchased from Gibco, and trypsin-EDTA, MTT, and trypan blue were provided by Sigma-Aldrich.

The toxicity of the nanostructure was determined using the MTT assay in the 4T1 cell line. For this purpose, after incubating *PpIX* (both free and loaded in nanomicelles) for 3 hr at six concentrations (0, 5, 10, 15, 20, and 30 µM), the percentage of cell viability was determined. The optimal concentration that resulted in more than 80% viability was selected for *in vivo* experiments.

Animals

Male BALB/c mice were purchased from the Pasteur Institute, Karaj Branch, Iran, and used at 6–8 weeks of age (n=30, mean weight 22 g). The animals were maintained under specific pathogen-free conditions at 22–25 °C with a 12 hr light/dark cycle. All animal procedures complied with the Animal Care and Use Committee-approved protocols of Mashhad University of Medical Sciences.

In vivo study of the effects of SDT

After culturing and proliferating 4T1 cells in RPMI-1640 medium supplemented with 10% FBS, the cells were harvested for injection into 8-week-old male inbred BALB/c mice. Before injection, the left flank hair of the animals was shaved, and 500,000 cells were subcutaneously injected to induce breast tumor models. The mice were then randomly divided into six groups (n=5 per group). For ultrasound (US) exposure, the Soleo Sono device (Zimmer Company) was used as the US source. Before treatment, the mice were anesthetized via intraperitoneal injection of 2% xylazine (6 mg/kg) and ketamine (60 mg/kg). Therapy was initiated when tumors reached a volume of 100 mm³. The device generates frequencies of 800 kHz and 2400 kHz in both continuous and pulsed modes. The output intensity ranges from 0.1 to 1 W/cm² (small probe) and 0.1 to 3 W/cm² (large probe). In US-treated groups, 10 min after intratumoral drug injection (15 μ M), tumors were exposed to dual-frequency US (800 + 2400 kHz) at 1 W/cm² intensity for 10 min.

Evaluating treatment efficacy

Evaluating the effect of treatment was done by measuring tumors' dimensions in all groups using a calliper. Measurements were continued up to 20 days after treatment. Then the mice were sacrificed, and the tumors were removed for pathological study and to determine the percentage of tumor necrosis in different groups. To calculate the lost volume, first, the volume lost through necrosis (v1) was obtained as the product of the percentage of necrosis in the remaining tumor volume on the last day. Also, the treatment-induced inhibition volume was calculated as the difference between the tumor volume on the day of treatment and the last day (v2). Finally, the total lost volume was estimated from the sum of v1 and v2.

Statistical analysis

Statistical analysis of the data was performed using SPSS version 26. The Kolmogorov-Smirnov test, one-way ANOVA, and the Mann-Whitney test were utilized to assess normality and compare data at a 95% confidence level.

Results

Characterization of PpIX-loaded nanomicelles

Spectrophotometric analysis: The absorbance spectra of free PpIX (dissolved in water) and micelles containing PpIX (with a dye concentration of 0.01 mM in both samples) are shown in Figure 1. In the PpIX-loaded nanomicelles, an absorbance peak is observed at approximately 410 nm, which is absent in free PpIX.

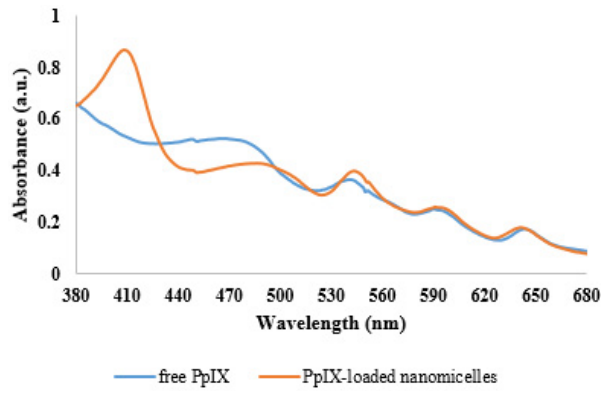
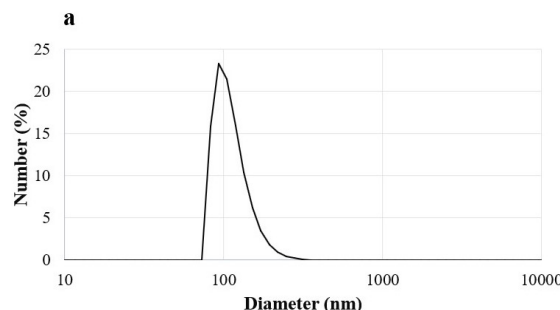


Figure 1. UV-Visible spectra of free PpIX and PpIX-loaded nanomicelles (with a dye concentration of 0.01 mM in both). PpIX: Protoporphyrin IX

DLS analysis revealed that the PpIX-loaded nanomicelles exhibited a mean hydrodynamic diameter of 106 nm (Figure 2a) with a polydispersity index (PDI) of 0.61 (Table 1). The zeta potential measurement indicated a near-neutral surface charge of -8 mV (Figure 2 b).

In vitro cytotoxicity assessment of PpIX

The percentage of cell viability at various concentrations of PpIX and PpIX-loaded nanomicelles (5, 10, 15, 20, and 30 μ M) is presented in Figure 3. Free PpIX did not cause a

Table 1. Characterization data of protoporphyrin IX (PpIX)-loaded nanomicelles

Parameter	Value
Hydrodynamic diameter (nm)	106 \pm 12
Polydispersity index (PDI)	0.61 \pm 0.08
Zeta potential (mV)	-8 \pm 2

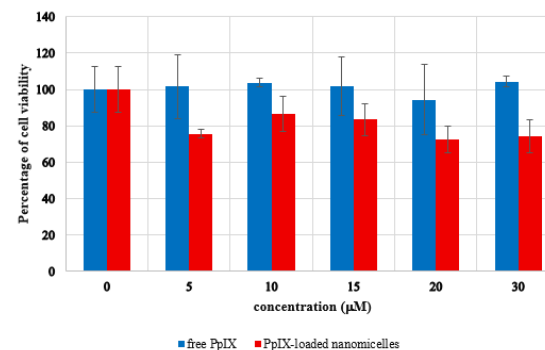


Figure 3. In vitro cytotoxicity of PpIX (0–30 μ M) after 3 hr incubation in 4T1 murine mammary carcinoma cells, assessed by MTT assay. Data represent mean \pm SD (n = 3). PpIX: Protoporphyrin IX

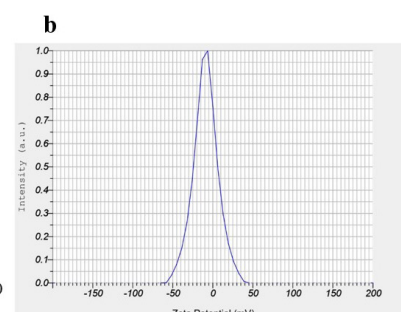


Figure 2. Dynamic light scattering measurements (DLS) of PpIX-loaded nanomicelles (peak: 88.8 nm) and Zeta potential measurements (peak: -8 mV). PpIX concentration: 0.01 mM; surfactant to water ratio: 2.5 mM. PpIX: Protoporphyrin IX

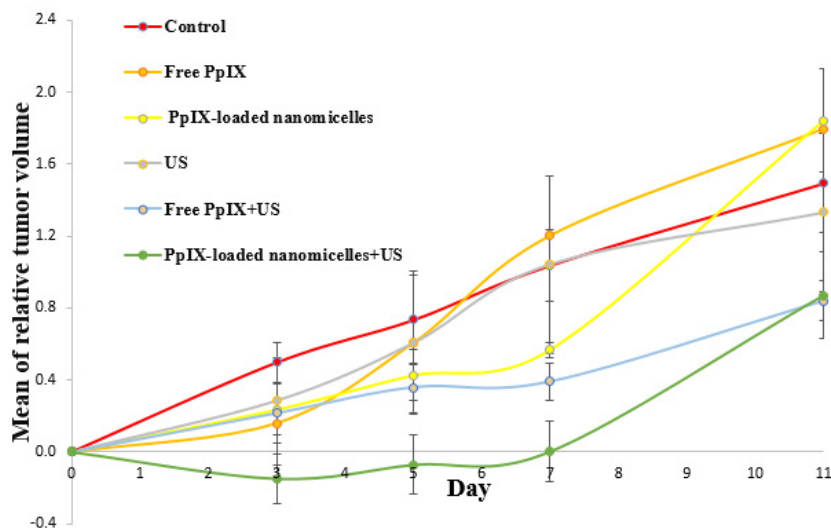


Figure 4. Mean of relative tumor volume until 11 days post-treatment in different mouse groups

Control, treated with 100 μ l physiological serum; free PpIX, treated with 100 μ l PpIX at concentration 15 μ M; PpIX-loaded nanomicelles, treated with 100 μ l PpIX at concentration 15 μ M; US, tumors irradiated with ultrasound wave alone; free PpIX+US, tumors irradiated with ultrasound wave 10 min after injection of 100 μ l PpIX at concentration 15 μ M; PpIX-loaded nanomicelles+US, tumors irradiated with ultrasound 10 min after injection of 200 μ l PpIX at concentration 15 μ M. Data represent mean \pm SEM (n = 5).

PpIX: Protoporphyrin IX

significant reduction in cell viability at any concentration. However, PpIX-loaded nanomicelles significantly reduced cell viability at concentrations of 5, 20, and 30 μ M compared to the control group (no drug). Based on these results, a concentration of 15 μ M was selected for further studies.

In vivo effect of SDT

Relative tumor volume variations up to 11 days post-treatment in different groups are presented in Figure 4. The Kolmogorov-Smirnov test indicated that the data on relative tumor volumes at different days post-treatment did not follow a normal distribution. Additionally, a preliminary analysis confirmed that there were no significant differences in tumor dimensions on the treatment day (100 cm^3). Due to mortality beyond day 11, the mean relative tumor volume for each group was calculated for the first 11 days post-treatment and compared using the Mann-Whitney U test at a 95% confidence level. As shown in Figure 4, a significant difference was observed between the SDT group, mediated by PpIX-loaded nanomicelles, and the control group, the free PpIX group, and the ultrasound-alone group ($P < 0.05$). Additionally, the SDT group using free PpIX showed a significant difference compared to the control group ($P < 0.05$).

Percentage of tissue volume lost

The average volume of tissue loss across groups is shown in Figure 5. Negative values in the graph indicate an increase in relative tumor volume. As observed, the control group and the groups receiving free PpIX or PpIX-loaded nanomicelles show no increase in volume and no decrease in tissue volume. The greatest increase in tumor volume was observed in the control group, whereas the greatest reduction in tumor volume was observed in the SDT group treated with PpIX-loaded nanomicelles.

Discussion

SDT is an adjuvant cancer treatment method with a controllable depth of penetration and minimal side effects (21). In SDT, the cytotoxic effects of drugs (sonosensitizers) on tumor cells are enhanced by ultrasound exposure.

This approach leverages both physical effects (such as mechanical stress and cavitation) and biochemical effects (such as reactive oxygen species, ROS) to induce cellular damage and apoptosis, and inhibit tumor growth. However, most sonosensitizers are hydrophobic, leading to their aggregation in biological environments, reduced water solubility, and diminished ROS production. Additionally, many sonosensitizers exhibit poor pharmacokinetic properties and are rapidly cleared from the vascular system, which limits their presence at pathological sites. Furthermore, their non-specific biological distribution and poor selectivity result in only a small fraction reaching the target sites. This insufficient intracellular concentration of sonosensitizers may fail to induce a therapeutic effect (21). On the other hand, nanomicelles, due to their small size, good biocompatibility, and ability to encapsulate lipophilic drugs in their core, have demonstrated their effectiveness as nanocarriers in drug delivery (22). It should be noted that the relatively neutral charge of the nanomicelles can be attributed to the nonionic nature of the surfactants used in the formulation.

In the present study, nanomicelles containing the sonosensitizer PpIX were prepared, and the sonodynamic effects mediated by these nanostructures were investigated in a 4T1 breast tumor model in BALB/c mice. The synthesized nanomicelles enhanced the PpIX absorbance peak at 410 nm. Given that the sonoluminescence spectrum, light emission from collapsing bubbles in a liquid induced by ultrasound, exhibits maximum intensity in the violet and blue region, its intensity decreases exponentially with increasing wavelength (23). It appears that the synthesized nanomicelles can increase sonoluminescence efficiency, thereby improving the therapeutic effects of SDT. Additionally, by enhancing the drug absorbance peak at a wavelength corresponding to the sonoluminescence peak, these nanostructures may also enable cells to benefit from PDT. Liu *et al.* used micelles loaded with the sonosensitizer hypocrellin and observed uniform distribution of hypocrellin in the tumor after ultrasound irradiation. They also reported a significant increase in ROS levels and subsequent cell death (17).

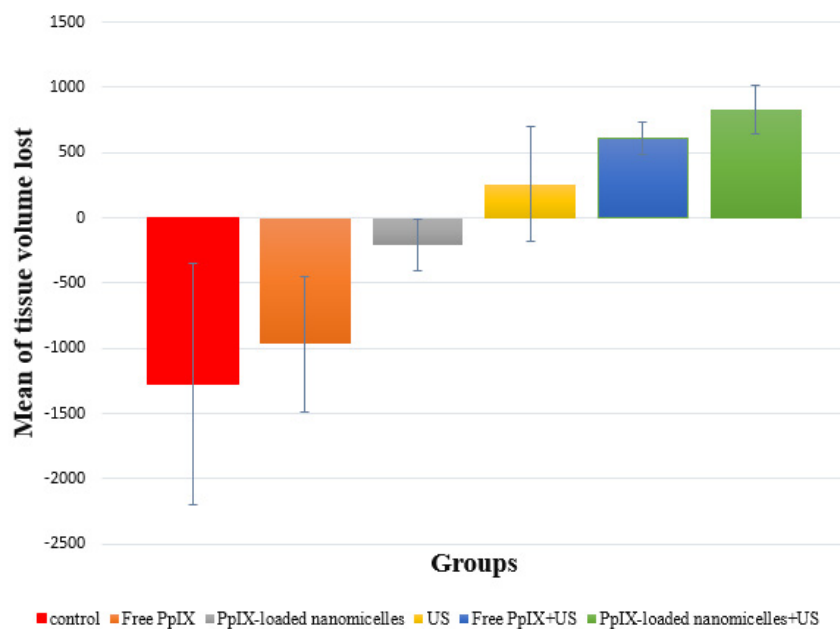


Figure 5. Percentage of lost tissue volume in mouse treatment groups

Control, treated with 100 μ l physiological serum; Control, treated with 100 μ l physiological serum; free PpIX, treated with 100 μ l PpIX at concentration 15 μ M; PpIX-loaded nanomicelles, treated with 100 μ l PpIX at concentration 15 μ M; US, tumors irradiated with ultrasound wave alone; free PpIX+US, tumors irradiated with ultrasound wave 10 min after injection of 100 μ l PpIX at concentration 15 μ M; PpIX-loaded nanomicelles+US, tumors irradiated with ultrasound 10 min after injection of 100 μ l PpIX at concentration 15 μ M. Data represent mean \pm SEM ($n = 5$). PpIX: Protoporphyrin IX

In this study, all groups achieved a relative reduction in tumor volume compared to the control group within the first seven days. However, this reduction was significant only in the groups treated with SDT mediated by PpIX-loaded nanomicelles or with free PpIX. These results may indicate the sonosensitizing effect of PpIX. Sazgarnia *et al.* also investigated the sonodynamic effect of PpIX conjugated with gold nanoparticles (GNP). Their results showed that the sonosensitizing effect depended on the concentration of the conjugate, with higher drug concentrations or irradiation intensities enhancing it (24). Similarly, Liu *et al.* compared the sonosensitizing effects of PpIX and hematoporphyrin (HP) and found that PpIX exhibited greater cytotoxic effects than HP (25).

Given that a reduction in tumor volume was observed on the fourth day post-treatment in the group treated with SDT mediated by PpIX-loaded nanomicelles, followed by tumor regrowth (Figure 4), it appears that repeating the treatment on the fourth day may inhibit tumor growth. Alamolhoda *et al.* investigated the effects of dose fractionation and repeated SDT with dual-frequency ultrasound on a mouse model of breast adenocarcinoma. They demonstrated that repeated ultrasound doses at two, three, and four sessions were more effective in delaying tumor growth compared to a single treatment. Additionally, dose fractionation significantly reduced tumor growth rate, even compared to four sessions of repeated ultrasound treatment (11). The greatest reduction in tumor volume was observed in the group treated with SDT mediated by PpIX-loaded nanomicelles (Figure 5). Martins *et al.* conducted a similar study investigating the effects of SDT on micelles loaded with zinc phthalocyanine (ZnPc@ Micelle). The measured cavitation and ROS levels in the ZnPc@Micelle group increased with prolonged irradiation time. The micelles also enhanced the stability of the sonosensitizer and increased drug release by up to 40-fold after ultrasound irradiation compared to the non-irradiated group (15). They concluded that the increased stability of

ZnPc and its enhanced release upon ultrasound irradiation could be attributed to its encapsulation within nanomicelles (16). In the present study, intratumoral delivery was used to achieve localized delivery and directly assess the therapeutic efficacy of PpIX-loaded nanomicelles in a controlled tumor model. For clinical applicability, however, systemic delivery (e.g., intravenous injection) represents a more feasible and patient-compliant delivery route. Future research should therefore examine the pharmacokinetics, biodistribution, and tumor accumulation of PpIX nanomicelles following systemic delivery.

By virtue of their nanoscale size (~100 nm) and almost neutral surface charge (~-8 mV), the nanomicelles will likely benefit from the EPR effect to accumulate passively in tumor tissue via leaky tumor vasculature and compromised lymphatic drainage. Physicochemical factors, such as particle size, surface charge, and hydrophilicity, can also be optimized to enhance EPR-based targeting efficiency.

Furthermore, active targeting strategies (e.g., conjugation with tumor-specific ligands or antibodies) can be explored to complement EPR-mediated accumulation and reduce off-target distribution. These studies will establish the feasibility of systemic administration and the translational potential of PpIX-loaded nanomicelles as clinically feasible sonosensitizer delivery systems for SDT (26, 27).

Conclusion

Based on this study's results, PpIX appears to be a suitable sonosensitizer. Using nanomicelles as a drug delivery system for PpIX not only enhances its solubility and uniform distribution but also increases cavitation efficiency under ultrasound irradiation. Furthermore, this nanomicellar structure, by amplifying the optical absorption peak of PpIX in the region corresponding to the sonoluminescence spectrum, may enable simultaneous PDT during SDT, thereby improving treatment efficacy. Therefore, by employing dosimetry methods and identifying the types of

free radicals generated in the environment, the concurrent occurrence of PDT and SDT should be assessed.

It is evident that a single treatment session is insufficient to completely inhibit tumor growth, and repeated treatments are necessary. By repeating the treatment on the fourth day, it is expected that the tumor growth rate will be reduced.

In summary, this study provides preliminary evidence of the effectiveness of SDT mediated by dual-frequency US and PpIX-loaded nanomicelles in a breast tumor model in BALB/c mice.

Acknowledgment

This study (ID: 4001867) was registered with and financially supported by the Vice Chancellery for Research of Mashhad University of Medical Sciences and the Vice Chancellery for Research of Torbat Heydarieh University of Medical Sciences (Grant ID: 401000037). We are sincerely grateful to the dean of the Medical Physics Research Center at Mashhad University of Medical Sciences for providing the opportunity to conduct this study.

Authors' Contributions

A S and B KN designed the experiments; M B, B KN, S SS, M H, and N TM performed the experiments and collected the data; A S and M B analyzed, interpreted, and discussed the results and strategy; M B, A S, B KN, and M H drafted the manuscript and critically reviewed the article; A S supervised, directed, and managed the study; A S, M B, B KN, M H, S SS, and N TM gave final approval for the version to be published.

Conflicts of Interest

The authors declare that no conflict of interest exists.

Declaration

We acknowledge the use of DeepSeek for English grammar correction to enhance the clarity and readability of this manuscript. All scientific content, including concepts, data analysis, interpretations, and conclusions, was generated and validated solely by the authors without the use of AI for content creation.

References

- Mattiuuzzi C, Lippi G. Current cancer epidemiology. *J Epidemiol Glob Health* 2019; 9:217-222.
- Miller KD, Nogueira L, Mariotto AB, Rowland JH, Yabroff KR, Alfano CM, et al. Cancer treatment and survivorship statistics, 2019. *CA Cancer J Clin* 2019; 69:363-385.
- Hong L, Pliss AM, Zhan Y, Zheng W, Xia J, Liu L, et al. Perfluoropolyether nanoemulsion encapsulating chlorin e6 for sonodynamic and photodynamic therapy of hypoxic tumor. *ACS Appl Mater Interfaces* 2020; 10:2058-2070.
- Xiong X, Zheng L-W, Ding Y, Chen Y-F, Cai Y-W, Wang L-P, et al. Breast cancer: Pathogenesis and treatments. *Signal Transduct Target Ther* 2025;10:49-81.
- Zheng Y, Ye J, Li Z, Chen H, Gao Y. Recent progress in sono-photodynamic cancer therapy: From developed new sensitizers to nanotechnology-based efficacy-enhancing strategies. *Acta Pharm Sin B* 2021; 11:2197-2219.
- Wang X, Zhang W, Xu Z, Luo Y, Mitchell D, Moss RW. Sonodynamic and photodynamic therapy in advanced breast carcinoma: A report of 3 cases. *Integr Cancer Ther* 2009; 8:283-287.
- Miller DL, Smith NB, Bailey MR, Czarnota GJ, Hynynen K, Makin IR. Overview of therapeutic ultrasound applications and safety considerations. *J Ultrasound Med* 2012; 31:623-634.
- Datta P, Moolayadukkam S, Chowdhury D, Rayes A, Lee NS, Sahu RP, et al. Recent advances and future directions in sonodynamic therapy for cancer treatment. *BME Front* 2024;2024:0080.
- Rosenthal I, Sostaric JZ, Riesz P. Sonodynamic therapy—a review of the synergistic effects of drugs and ultrasound. *Ultrason Sonochem* 2004; 11:349-363.
- Shen Y, Pflieger R, Chen W, Ashokkumar M. The effect of bulk viscosity on single bubble dynamics and sonoluminescence. *Ultrason Sonochem* 2023; 93:106307.
- Alamolhoda M, Mokhtari-Dizaji M. Evaluation of fractionated and repeated sonodynamic therapy by using dual frequency for murine model of breast adenocarcinoma. *Ultrasonics* 2015; 58:77-85.
- Adelnia A, Mokhtari-Dizaji M, Hoseinkhani S, Bakhshandeh M. The effect of dual-frequency ultrasound waves on B16F10 melanoma cells: Sonodynamic therapy using nanoliposomes containing methylene blue. *Skin Res Technol* 2021;27:376-384.
- Yamaguchi T, Kitahara S, Kusuda K, Okamoto J, Horise Y, Masamune K, et al. Current landscape of sonodynamic therapy for treating cancer. *Cancers* 2021; 13:6184-6195.
- Martins YA, Pavan TZ, Lopez RFV. Sonodynamic therapy: Ultrasound parameters and *in vitro* experimental configurations. *Int J Pharm.* 2021; 610:121243.
- Yan P, Liu LH, Wang P. Sonodynamic therapy (SDT) for cancer treatment: Advanced sensitizers by ultrasound activation to injury tumor. *Adv Biosyst* 2020; 4:e2000123.
- Martins YA, Fonseca MJ, Pavan TZ, Lopez RF. Bifunctional therapeutic application of low-frequency ultrasound associated with zinc phthalocyanine-loaded micelles. *Int J Nanomedicine* 2020; 15:8075-8095.
- Liu X, Zhao K, Cao J, Qi X, Wu L, Shen S. Ultrasound responsive self-assembled micelles loaded with hypocrellin for cancer sonodynamic therapy. *Int J Pharm* 2021; 608:121052.
- Son S, Kim JH, Wang X, Zhang C, Yoon SA, Shin J, et al. Multifunctional sonosensitizers in sonodynamic cancer therapy. *Chem Soc Rev* 2020; 49:3244-3261.
- Hoseini M, Sazgarnia A, Sharifi S. Effect of environment on protoporphyrin IX: Absorbance, fluorescence and nonlinear optical properties. *J Fluoresc* 2019;29:531-540.
- Pellosi DS, Moret F, Fraix A, Marino N, Maiolino S, Gaio E, et al. Pluronic® P123/F127 mixed micelles delivering sorafenib and its combination with verteporfin in cancer cells. *Int J Nanomedicine* 2016;11:4479-4494.
- Huang Y, Ouyang W, Lai Z, Qiu G, Bu Z, Zhu X, et al. Nanotechnology-enabled sonodynamic therapy against malignant tumors. *Nano Today* 2024; 54:102145.
- Tawfik SM, Azizov S, Elmasry MR, Sharipov M, Lee YI. Recent advances in nanomicelles delivery systems. *Nanomaterials* 2020; 11:70-103.
- Gaitan D, Atchley A, Lewia S, Carlson J, Maruyama X, Moran M, et al. Spectra of single-bubble sonoluminescence in water and glycerin-water mixtures. *Phys Rev E* 1996; 54:525-528.
- Sazgarnia A, Shafei A, Meibodi NT, Eshghi H, Nassirli H. A novel nanosonosensitizer for sonodynamic therapy: *In vivo* study on a colon tumor model. *J Ultrasound Med* 2011; 30:1321-1329.
- Liu Q, Wang X, Wang P, Xiao L, Hao Q. Comparison between sonodynamic effect with protoporphyrin IX and hematoporphyrin on sarcoma 180. *Cancer Chemother Pharmacol* 2007; 60:671-680.
- Ravera S, Bertola N, Pasquale C, Bruno S, Benedicenti S, Ferrando S, et al. 808-nm photobiomodulation affects the viability of a head and neck squamous carcinoma cellular model, acting on energy metabolism and oxidative stress production. *Biomedicines* 2021; 9:1717-1732.
- Kang M, Lee Y, Lee Y, Kim E, Jo J, Shin H, et al. Wavelength-dependent photobiomodulation (PBM) for proliferation and angiogenesis of melanoma tumor *in vitro* and *in vivo*. *J Photochem Photobiol B* 2024; 258:112990.